

# Experimental Methods to Study the Mechanisms of Interaction of Lipid Membranes with Low-Molecular-Weight Drugs

I. M. Le-Deygen<sup>a, 1</sup>, A. A. Skuredina<sup>a</sup>, and E. V. Kudryashova<sup>a</sup>

<sup>a</sup>Chemistry Department, Moscow State University, Moscow, 119991 Russia

Received February 8, 2020; revised February 20, 2020; accepted February 22, 2020

**Abstract**—The review is devoted to methods for studying how lipid membranes interact with low-molecular-weight drugs. The following methods are considered in the review: IR and EPR spectroscopy, fluorescence analysis, differential scanning calorimetry, and microscopy methods. Methods for characterizing the size and charge of vesicles are also considered: dynamic light scattering and nanoparticle tracking analysis. Methods are divided into those requiring additional labels and label-free. An important objective of the review is to find the optimal research strategy by selecting informative, modern approaches to studying the interactions of drugs with lipid membranes, as well as analyze the latest achievements of instrumental methods.

**Keywords:** liposomes, IR spectroscopy, EPR spectroscopy, fluorescence methods, differential scanning calorimetry

**DOI:** 10.1134/S1068162020040123

## INTRODUCTION

The development of new biologically active compounds and dosage forms poses significant questions for modern science related to the safety and efficiency of therapy. Incorporation of the active substances in lipid-based delivery systems allows one to combat the pronounced side effects of drugs and increases bioavailability and biocompatibility of the drugs. Thus, elucidation of the drug–membrane interaction and the effect of the active molecule on physicochemical properties of the bilayer are among the key tasks in creating new dosage forms.

The toolkit of physicochemical methods used for these purposes is extensive. However, an avalanche-like increasing number of publications on this issue necessitates a deep analysis of the accumulated data in order to discover new complex approaches to studying the interaction of lipid membranes with low-molecular-weight drugs.

This review is devoted to the analysis of the latest achievements of instrumental methods for studying

lipid systems. Methods that require a label and label-free ones are considered separately. Methods that do not require the introduction of a label include classical approaches, such as differential scanning calorimetry (DSC), atomic force microscopy (AFM), scanning electron microscopy (SEM), and cryoelectron microscopy, and relatively new ones, for example, the small-angle X-ray scattering, Fourier transform infrared spectroscopy, environmental scanning electron microscopy, and free electron laser diffraction.

Among the methods requiring the introduction of an additional label, fluorescence-based methods are considered, including fluorescence polarization analysis, time-resolved fluorescence anisotropy (TRFA), fluorescence correlation spectroscopy (FCS), and EPR spectroscopy.

Using a combination of the above methods, it is possible to assess the location and state of the drug in a liposome and to determine its binding sites and the effect of the active molecule on the phase transition and vesicle morphology.

Separately considered are the methods of lipid vesicles “quality control,” evaluation of the efficiency of loading of the active substance, determination of the size and charge of the vesicles: dynamic light scattering (DLS) and nanoparticle tracking analysis (NTA), chromatography-based methods, and UV and fluorescence spectroscopy. When considering this aspect, it is necessary to take into account the significant influence of the method for vesicle production on their physicochemical properties.

Abbreviations: 16-DSEA, 16-doxylstearic acid; 5-DSEA, 5-doxylstearic acid; AFM, atomic force microscopy; DPPC, dipalmitoylphosphatidylcholine; DSC, differential scanning calorimetry; DLS, dynamic light scattering; CL, cardiolipin; MR, mass ratio; SAXS, small angle X-ray scattering; ATIR, attenuated total internal reflection; NTA, nanoparticle tracking analysis; TRFA, time-resolved fluorescence anisotropy; HFI, hyperfine interaction; HFS, hyperfine splitting; SEM, scanning electron microscopy; FCS, fluorescence correlation spectroscopy; LE, loading efficiency; ESEM, environmental scanning electron microscopy.

<sup>1</sup> Corresponding authors: e-mail: i.m.deygen@gmail.com.

An important objective of the review, in addition to analyzing the latest achievements of instrumental methods of analysis, is to find the optimal research strategy by selecting informative, modern approaches to studying the interaction of drugs with lipid membranes.

### METHODS FOR QUALITY CONTROL OF VESICLES LOADED WITH A DRUG

Preparation of lipid vesicles loaded with a drug is a well-established procedure [1]. Methods for control of the resulting liposomal formulations are needed; usually, the homogeneity of the vesicles should be confirmed, their hydrodynamic radius and zeta potential should be determined, and the efficacy of drug inclusion should be evaluated. The methods considered in this section typically precede the analysis of the obtained liposome systems by other methods to establish how the drug–membrane interaction works.

#### *Methods to Determine the Size, Charge, and Homogeneity of Vesicles*

**Dynamic light scattering.** The classical method for determining the size of liposomes is dynamic light scattering [2]. This method allows one to obtain data on the size distribution of nano- and submicron particles in dilute solutions. A laser beam passing through a solution and reaching a particle is reflected and scattered, because its size is comparable to the wavelength. Continuous Brownian motion of particles leads to a constant movement of scattering sources. The fluctuation of the local particle concentration corresponds to the fluctuation of the intensity of the scattered light [3]. Based on the data of temporal fluctuations in the intensity of scattered light (Fig. 1a), an autocorrelation curve  $G(\tau)$  is constructed (Fig. 1b), which is described by Eq. (1):

$$G(\tau) = b[1 + \varepsilon \exp(-\tau/\tau_c)], \quad (1)$$

where the base (“random”) correlation level  $b$  is proportional to the total intensity  $I$ .

The diffusion coefficient  $D$  of the particles is inversely proportional to the decay time  $\tau_c$  of the considered correlation function:

$$D = \frac{1}{2\tau_c k^2}, \quad (2)$$

where  $k$  is a constant (modulus of the scattering wave vector).

The hydrodynamic radius of the nanoparticle is calculated using the Stokes–Einstein equation through the diffusion coefficient (3),

$$D = \frac{k_B T}{6\pi\eta r}, \quad (3)$$

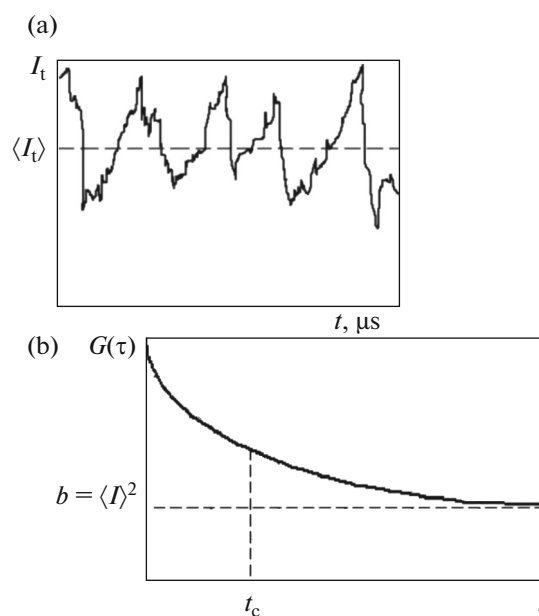


**Fig. 1.** Schematic representation of (a) fluctuations in the scattered light intensity recorded in a small volume in the microsecond-time interval and (b) corresponding auto-correlation function  $G(\tau)$ .

where  $D$  is the diffusion coefficient,  $k_B$  is the Boltzmann constant,  $T$  is the absolute temperature,  $\eta$  is the viscosity of the liquid, and  $r$  is the radius of the particle.

The method has entered the routine toolkit of liposome researchers [4], and it is difficult to imagine a reliable study on the interaction of membranes with drugs without the data on hydrodynamic radius and polydispersity index (PdI) of the liposomes [5].

DLS allows the study of suspensions of particles with sizes ranging from a few nanometers to microns. The method, however, has a number of significant limitations. Firstly, the presence of large micron-sized particles (dust particles, aggregates) in the suspension can distort the measurement results. For real systems, the limiting accuracy of measurements usually allows one to determine only the average particle size, width, and asymmetry of the particle size distribution. It is possible to “resolve” the peaks corresponding to two populations of vesicles of different sizes if the diameters differ 2–3-fold. For example, using DLS, it was possible to prove the formation of a population of small vesicles with a diameter of about 100 nm during incubation of giant monolamellar liposomes (diameter of about 2000 nm) with ATP and GTP for 15 min [6]. If there are populations of polymer-coated and uncoated liposomes in the system, most often two independent peaks cannot be detected, but a shift of the main maximum towards larger sizes is observed [7]. So, for anionic liposomes of  $60 \pm 2$  nm, coating with the polycation PEG–chitosan led to an increase in the hydrodynamic radius to  $85 \pm 4$  nm. If the task is

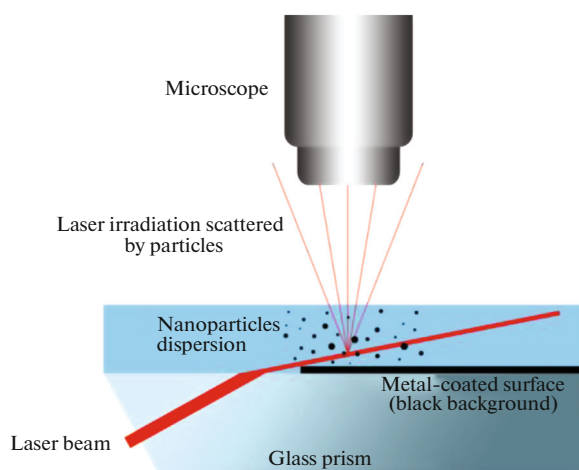


**Fig. 2.** Scheme of nanoparticle tracking analysis equipment.

to separate two populations of vesicles with close sizes, nanoparticle tracking analysis can be used.

**Nanoparticle tracking analysis (NTA).** This approach is often used to determine the concentration of nanoparticles in solution and their size distribution. The solution is irradiated with a laser, while particles smaller than a wavelength behave like point light scatterers. Observation is made through an ultramicroscope located on top, at a right angle to the laser. A highly sensitive camera records video of the particles' Brownian motion. Next, based on the known volume of the observation region and the number of registered particles, the computer calculates the concentration of particles in the solution (Fig. 2) [8]. For example, according to NTA, in a suspension of anionic liposomes consisting of 80% dipalmitoylphosphatidylcholine (DPPC) and 20% cardiolipin (CL) by weight, a total lipid concentration of 3 mg/mL contains  $1 \times 10^{16}$  vesicles/L [9], which is consistent with theoretical calculations. This made it possible to determine the number of polymer molecules per each liposome in a complex of liposomes with PEG chitosan.

As in the dynamic light scattering method, the hydrodynamic radius of a nanoparticle is calculated by the Stokes–Einstein equation. The advantages of NTA include the ability to distinguish between populations of vesicles with a small difference in size (20–30%), the ability to work with very low concentrations of the sample (usually  $10^6$ – $10^9$  particles/mL), and the ability to exclude the factor of large dust particles or aggregates. On the other hand, sample preparation in the NTA method requires the use of high-purity water (usually the Milli-Q system is used, in which water passes through ion-exchange resins and activated carbon cartridges, and then through filters with a pore size of 0.22 microns, so that the resistivity is 18.2 MΩ cm). However, work at high dilutions (in the case of a suspension of liposomes of 3 mg/mL, it is necessary to

dilute the sample at least 10000 times) can lead to the dissociation of noncovalent liposomal complexes, which, as a rule, have dissociation constants of the order of  $10^{-4}$  M.

DSL and NTA methods are compared in [10]. A suspension of cationic liposomes made of egg phosphatidylcholine–1,2-dioleoyl-*sn*-glycero-3-phosphoethanolamine–1,2-dioleoyl-3-trimethyl ammonium propane, 4 : 2 : 1 by mole, was analyzed. According to DLS, the average hydrodynamic diameter was 117 nm with a polydispersity index of 0.248, which indicates the heterogeneity of the vesicle population. However, according to the NTA, the liposomes were larger (154 nm) and more homogeneous.

The discrepancy between the results of liposome size determination by DLS and NTA is often observed [11], which is associated with a fundamental difference in the physical basis of the methods. At the same time, it is not possible to unequivocally reject or recommend one method or another to solve routine problems, since both approaches have a number of limitations. In the case of DSL, the hydrodynamic radius is usually taken into account, and for additional information, a size distribution weighted by intensity and number of particles is considered, which allows one to reveal the effect of large aggregates. In NTA, the most informative is the comprehensive analysis of the trajectory of each particle in the video recording, including the analysis of the full length of the trajectory of the vesicle (finite track length adjustment, FTLA) for the most correct selection of trajectories in the calculation of the hydrodynamic radius.

The best solution may be a combination of both methods, as, for example, in [12]. Additional information on the size of liposomes can be obtained using electron microscopy methods, which will be discussed in the following sections of the review.

**Determination of the  $\zeta$ -potential of liposomes.** Often, DSL devices are equipped with the ability to measure the  $\zeta$ -potential of vesicles (sometimes called the electrokinetic potential). This concept is introduced when considering the double electric layer of a moving colloidal particle (Fig. 3) and it is convenient to use it to both estimate the charge of liposomes and make assumptions about their stability. It is known that charged vesicles aggregate more slowly, and their surface is easier to functionalize with polymers for use in targeted delivery systems [7, 13, 14]. It should be noted that the  $\zeta$ -potential is very sensitive to changes in conditions: the value is affected by pH, ionic strength, temperature, etc.

The  $\zeta$ -potential is measured in a special cell equipped with two electrodes. Applied electric field drives charged vesicles with a speed proportional to the  $\zeta$ -potential. The speed (electrophoretic mobility,  $U_e$ ) is determined by light scattering. The calculation of

the  $\zeta$ -potential is carried out according to Henry's equation (4):

$$U_e = \frac{2\varepsilon\zeta f(\kappa a)}{3\eta}, \quad (4)$$

where  $\varepsilon$  is the dielectric constant,  $\eta$  is the viscosity of the medium,  $f(\kappa a)$  is the Henry function,  $\kappa$  is the Debye length of the particle, and  $a$  is the Debye radius of the particle. In the Smoluchowski approximation for aqueous media, the Henry function is taken equal to 1.5, and in nonaqueous media, 1.

A comparative analysis of the  $\zeta$ -potential of liposomes of various lipid compositions and charge was performed in [15]. By varying the content of anionic or cationic lipid in the neutral matrix, the authors found a linear dependence of the  $\zeta$ -potential on the molar content of the charged lipid. In [9, 16], gradual neutralization of the  $\zeta$ -potential of anionic liposomes with saturation was demonstrated upon addition of polycations, derivatives of chitosan. Incorporation of drug molecules into the bilayer or inner water volume rarely can significantly affect the total charge of the vesicles: small changes are described in the literature, most often within the confidence interval [17, 18].

It should be noted that in addition to the  $\zeta$ -potential, a related parameter, electrophoretic mobility, is often used to estimate the surface charge of particles [14]. This value is measured by laser microelectrophoresis. For example, when studying the interaction of polycations with liposomes based on egg lecithin and cardiolipin with the initial negative value of electrophoretic mobility, polymer sorption led to complete charge neutralization, and further sorption led to recharging of the vesicle surface.

The group of methods for determining the size, charge, and homogeneity of vesicles considered above, therefore, not only serves to control the quality of the resulting vesicles, but also provides valuable information on particle populations. Changing the particle size or their charge upon incorporation of a drug can provide evidence in favor of one or another mechanism of interaction of the active molecule with the bilayer.

#### *Methods for Determination of Drug Loading Efficiency*

A key characteristic of liposomes as drug delivery systems is the loading efficiency (LE) of the active molecule. Two parameters are to be distinguished: the actual LE, calculated as the ratio of the mass (or moles) of the incorporated drug to the total drug mass (or moles) added to the lipid suspension, and the drug–lipid mass ratio (MR) in the obtained liposomal formulation. Both parameters are important characteristics of a delivery system: LE is suitable for comparing different loading methods of the same drug, while MR is more important when comparing liposome delivery systems with other carriers in optimiz-

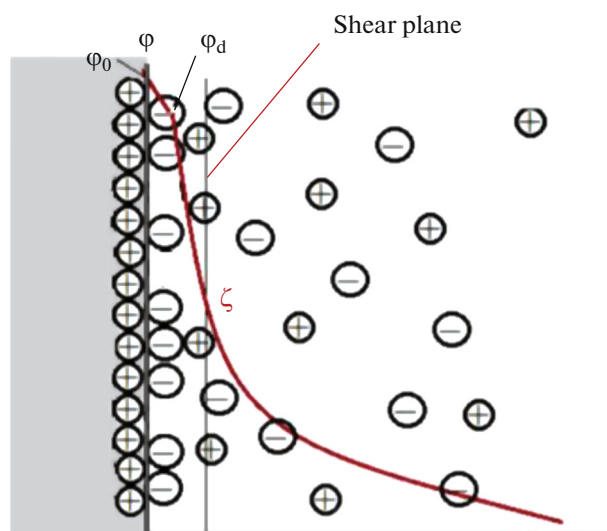


**Fig. 3.** Structure of the electric double layer: the shear plane potential corresponds to the electrokinetic  $\zeta$ -potential of the vesicle. In the figure,  $\varphi_0$  is the surface potential and  $\varphi_d$  is the Stern potential.

ing the ratio of drug mass to the total mass of the delivery system. Thus, both of these parameters often need to be calculated. Usually, the initially added amount of the drug is known, so it is necessary either to determine the drug content in liposomes, or to determine the content of unincorporated drug. The general scheme to determine LE is presented in Fig. 4.

Methods for determination of the amount of unincorporated drug are more common. Dialysis or gel permeation chromatography is usually used to separate the liposomal fraction from the free drug. The advantages and disadvantages of these methods are reflected in Table 1. Both methods are rightly actively used in research practice.

The drug content in the washings (in the case of dialysis) or in fractions free from liposomes is determined. The choice of analytical method is mainly based on the nature of the active molecule: UV spectroscopy, high performance liquid chromatography, and fluorescence methods are often used. For some drugs, for example, rapamycin, high performance liquid chromatography is practically the only possible solution due to the lack of analytically significant UV and fluorescence spectra [19]. The use of IR spectroscopy is acceptable if the content of the active molecule in the studied fraction is not less than 0.2–0.5 mg/mL in view of the detection limit of the method.

When liposomes are destroyed by detergent, the same methods are used to determine the drug content, adjusted for a possible change in the signal from the active molecule. For example, when destroying liposomes loaded with doxorubicin with the Triton-X surfactant, it is necessary to determine the drug content using calibration curves obtained for the drug in the



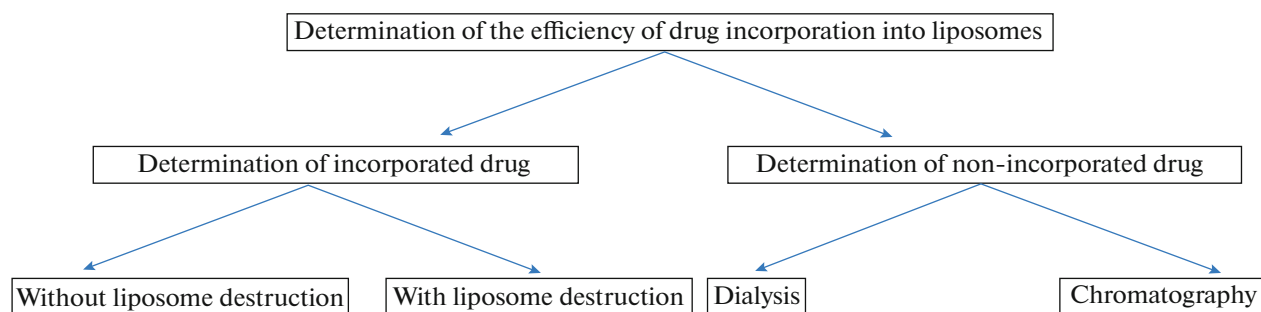


Fig. 4. Methods to determine the efficiency of drug incorporation into liposomes.

presence of the corresponding detergent content, since potential micelle formation [20] can significantly change the molar absorption coefficient of the drug and distort the results of LE determination.

Methods for determination of LE in liposomes without preliminary destruction are much less developed. This is due to several reasons: first, liposomal systems are often optically opaque, which makes it difficult to use many spectral methods. Secondly, the presence of lipids per se and their colloidal vesicles can significantly distort the signal from the active molecule.

#### METHODS FOR STUDYING MECHANISMS OF INTERACTION OF A LIPID BILAYER AND A DRUG

##### *Methods for Studying Lipid Systems that Require No Label*

The methods considered above are primarily used to control the quality of the obtained liposomal formulations of active molecules, but do not provide information on the mechanism of drug–bilayer interaction. Below are the methods that may be useful for studying the basic laws of this process. Their important advantage is the lack of the need to introduce additional labels in the bilayer, which simplifies the interpretation of data and speeds up the analysis.

**Differential scanning calorimetry.** Let us consider in more detail the method of differential scanning calorimetry, which initially found its wide application in the study of phase transitions in liposomes. An

exhaustive review is given in [21], which describes the capabilities of DSCs for analyzing the structure and properties of liposomes, but the method is also well suited to establish the features of the interaction of low- and high-molecular-weight substances with a bilayer based on differences in calorimetric curves.

In [22], using the DSC method, it was found that during the interaction of the liposome membrane (100% distearoylphosphatidylcholine) with tamoxifen, the phase transition shifts to lower temperatures, while the maximum of the DSC curve broadens, which indicates membrane destabilization, apparently due to embedding drugs in the bilayer.

Accurate registration of DSC curves allows obtaining information about the state of the drug in liposomes and determining the localization of the drug. Foggia and colleagues studied the interaction of a nonsteroidal anti-inflammatory drug ibuprofen with liposomes made of dimistroylphosphatidylcholine [23]. Registration of DSC curves at various pH values made it possible to establish that the protonated form of ibuprofen at pH 3 is able to penetrate the nonpolar part of the bilayer, while at pH 7 the interaction of deprotonated ibuprofen with choline groups of phospholipids prevents further penetration of the drug.

Yechezkel Barenholz [24] and colleagues, when developing a new lipophilic prodrug of mitomycin C and studying its effect on the membrane of PEGylated liposomes, found that the presence of two stearic acid residues in the prodrug structure ensures stable incorporation into the liposome bilayer, as evidenced by a change in the maximum of the DSC curve: the peak

Table 1. Methods used to separate liposomal fraction from unincorporated drug

Method	Advantages	Disadvantages
Dialysis	Methodological simplicity Availability (dialysis bags with high molecular weight cutoff are suitable)	Liposome preservation should be controlled Strong dilution of the free drug fraction Duration: several hours to several days
Gel permeation chromatography	Methodological simplicity Rapidly Small sample volume (below 1 mL)	Column phase should be selected Liposomal fraction can be diluted

becomes highly intense and narrow with a maximum at 56°C and a shoulder at 53°C; in the case of control liposomes, the peak was wide with a maximum at 53°C. The authors note that this type of phase transition is characteristic of a membrane containing cholesterol and explain the observed phenomenon by the formation of prodrug-rich domains in membranes, in which hydrophobic chains are densely packed into highly ordered crystal-like structures.

The attention of researchers is drawn to the study of nanocrystals of drug molecules that are formed upon incorporation into liposomes [25]. Lee and colleagues focused on methods for producing such nanocrystalline systems in liposomes, mentioning DSC as a possible method for detecting crystals in vesicles. The crystallinity of doxorubicin sulfate and some other drugs was previously shown using high-resolution calorimetry, but there is a debate about their nature and properties. In 2012 [26], no significant effect of the incorporation of doxorubicin on the phase transition of dipalmitoylphosphatidylcholine liposomes was found. However, in 2017, an improved technique allowed Perinelli and colleagues to detect the ordered state of doxorubicin nanocrystals inside PEGylated liposomes (Doxil formulation), and the crystals remained stable even after heating to 80°C [27].

DSC allows one to monitor the microphase separation in the membrane of liposomes of mixed composition. Thus, for mixed anionic DPPC–CL (8 : 2) liposomes, a combination of DSC and IR spectroscopy revealed stratification in the lipid bilayer with the formation of two domains with different melting points [18]. The calorimetric curve of mixed liposomes was characterized by a wide phase transition with a peak at 39°C and a shoulder at 35°C, which corresponded to the melting of two DPPC/CL microphases with different component ratios. For such liposomes loaded with moxifloxacin, it was possible to prove the structuring and stabilization of the gel phase due to the electrostatic interaction of the amino group of the drug molecule with the negatively charged cardiolipin. The temperature of the main phase transition of liposomes loaded with moxifloxacin shifted by 3–5 degrees.

Thus, the DSC method allows one to study the details of the phase transition process in liposomes and the effect of drugs on it, as well as indirectly detect the formation of nanocrystals or the integration of a drug molecule in the bilayer.

DLS was proposed as an alternative to DSC [28], with the average count rate as the analytical signal. The inclusion of celecoxib in the dimistroylphosphatidylcholine liposomes led to a significant shift in the average temperature vs. growth rate curve to high temperatures. A comparison of the curves for loaded and free liposomes at pH 5.0 and 7.4 revealed that at both pH values the curves shifted uniformly, but the effect was more pronounced (calculated melting points were

21.7° and 20.7° compared to the control value for free liposomes of 22.0°) at neutral pH. The authors suggest that in an acidic environment the incorporation of celecoxib affects the cooperativity of the phase transition, and not the value of the phase transition temperature, while at pH 7.4 celecoxib disorders the membrane, which manifests itself in a loss of cooperativity and a decrease in the temperature of the phase transition.

**Small-angle X-ray scattering.** In the method of small-angle X-ray scattering (SAXS), the intensity of X-rays scattered by a sample is measured as a function of the scattering angle (0.1–5 degrees). A key advantage of this method, compared to classical X-ray methods, is its versatility for many types of nanomaterials and the ability to record spectra from samples, both in powder and in gel and liquid dispersion forms. SAXS equipment allows one to study averaged structural features from a sample of large volume, which can be useful when working with heterogeneous colloidal systems. This method is well suited for studying the interaction of membranes with drug molecules that crystallize in the inner cavity of vesicles.

An important advantage of SAXS is the ability to determine the shape of the vesicles. It is known that DLS and NTA provide information on the hydrodynamic radius of particles based on the assumption of their spherical shape, while liposomes containing elongated nanocrystals can also take an elliptical shape. An analytically valuable parameter derived from a SAXS spectrum is the scattering vector  $q$ ; processing the dependence of the scattering intensity on  $q$  by the Fourier transform method makes it possible to plot the distribution function of pair distances.

Significant progress in the study of liposomal forms of nanocrystals of antibiotics was achieved by Chipolla and Chen, University of Sydney. Their work is primarily devoted to the study of nanocrystals of ciprofloxacin, a broad-spectrum antibiotic of the fluoroquinolone series [25, 29, 30]. For example, using a combination of SAXS, cryoelectron microscopy, and depolarized dynamic light scattering, the authors were able to prove [30] the cylindrical shape of liposomes loaded with ciprofloxacin.

The disadvantages of the SAXS method include the weak signal accumulated from liposomal suspensions, the possible overlap of the spectra of vesicles and nanocrystals, and the potential destruction of the sample during the study.

X-ray methods are actively used to study liposomal forms of photosensitizer inorganic nanoparticles, for example, iridium nanoparticles [31], in order to confirm the maintenance of crystallinity of the inorganic fraction after incorporation into vesicles. However, the interaction of liposomes with inorganic nanoparticles is a separate topic worthy of a voluminous review and goes beyond the scope of the topic discussed in this paper.

**Fourier transform infrared spectroscopy.** Fourier transform infrared spectroscopy has deservedly entered the toolkit of the researchers of lipid systems as one of the most informative and accurate methods, which allows one to obtain unique information about the microenvironment of lipid functional groups, their interaction with various ligands, and phase transitions. The use of IR spectroscopy for the analysis of biosystems became possible with the development of equipment and methods of mathematical processing (Fourier transform) of the initial signal of the device, i.e., interferograms.

Let us consider three optical effects that ensure high accuracy of the Fourier transform IR spectroscopy method. The first of them is called the Jacquinot advantage. Its essence is that in the Fourier spectrometer scheme, in contrast to the classical dispersion spectrometer, there are no slits, so that all the source radiation reaches the detector. At a fixed resolution, the aperture of a Fourier spectrometer is 200 times higher than the aperture of a dispersion spectrometer.

The next effect is called the Fellgett advantage, or the multiplex factor. It is associated with the simultaneous registration of all frequencies in the spectrum. For example, in case of simultaneous registration and processing of the spectral interval of  $4000\text{ cm}^{-1}$  at a resolution of  $1\text{ cm}^{-1}$ , the signal-to-noise ratio for the Fourier spectrometer is 63 times higher, and the spectrum recording speed is 4000 times higher. At present, registration of one high-resolution spectrum suitable for fine analysis of spectral bands takes no more than two minutes, which, undoubtedly, is an important methodological advantage of the method.

The third effect is called the Connes advantage. The use of helium-neon lasers in IR spectrometers as internal standards for wavelengths and for controlling interferograms depending on the position of a moving mirror made it possible to significantly increase the accuracy of determining wave numbers. Currently, some devices are characterized by a resolution of  $0.01\text{ cm}^{-1}$ . Such machines require fine-tuning before each start-up, while routine measurements can be reliably carried out at a resolution of  $1\text{--}2\text{ cm}^{-1}$ .

To date, in the study of complex biological systems, the most widely used mode is the attenuated total internal reflection (ATR) [32]. The ATR phenomenon is based on the penetration of radiation from an optically denser medium (crystal  $n_1$ ) into a less dense medium (sample  $n_2$ ) to a certain depth (the so-called penetration depth  $dp$ ), approximately equal to the wavelength, when light is incident at an angle greater than the critical one; thus part of the incident radiation penetrates the sample at  $dp$  and is absorbed there. The critical angle is defined as the angle of incidence at which the angle of refraction is  $90^\circ$ ; its value depends on the coefficients  $n_1$  and  $n_2$ .

It should be noted that since  $dp$  is directly proportional to the radiation wavelength, in the long-wavelength region of the ATR spectrum, a higher intensity of absorption bands should be expected. If  $n_2/n_1$  is constant, then  $dp$  linearly depends on the wavelength. Most modern programs for the analysis of IR spectra offer the ATR-correction function, which linearly corrects the band intensities, bringing the spectrum to a shape close to the transmission spectrum.

The pioneering work on the use of FTIR spectroscopy for the analysis of protein and lipid systems belongs to Erik Goormaghtigh and his research team at the Free University of Brussels, Belgium. In his laboratory, numerous spectral registration protocols with the selection of optimal conditions (crystal type, number of scans, atmospheric compensation method, etc.) and methods for the spectra analysis have been developed.

The IR spectrum of phospholipids has the following characteristic peaks of functional groups: two bands of symmetric and asymmetric vibrations of hydrocarbon bonds, vibrations of the carbonyl group  $\text{C}=\text{O}$ , and vibrations of the phosphate and choline groups (Fig. 5). The full correlation of the absorption bands and the corresponding vibrations of dipalmitoylphosphatidylcholine is presented in Table 2. The position of the bands and their shape are sensitive to binding of the bilayer with ligands, hydrogen bond formation, aggregation and oxidation, etc. [7, 11, 18, 26, 33–37].

The bands in the regions  $2853 \pm 5$  and  $2926 \pm 5\text{ cm}^{-1}$  correspond to symmetric and asymmetric stretching vibrations of the  $\text{CH}_2$  group, and the band at  $1465 \pm 5\text{ cm}^{-1}$  (the so-called methylene formation frequency) corresponds to bending vibrations. Symmetric deformation vibrations of the  $\text{CH}_3$  group are characterized by an absorption band at  $1375 \pm 5\text{ cm}^{-1}$ . A change in the conformation of lipid chains is accompanied by a frequency shift of the absorption bands of  $\text{CH}_2$  groups, and these changes correlate with the number of *cis* isomers of unsaturated residues of hydrophobic tails. *cis*-Isomers are less densely packed than *trans* isomers; acyl chains can change their direction and size. The increase in mobility is accompanied by a high-frequency shift in the IR spectrum [7]. The effect on the phase transition produced by various drugs can be evaluated both by the shift of the absorption bands of symmetric and asymmetric stretching vibrations of the  $\text{CH}_2$  groups and using the principal component analysis (PCA) method. The classic approach is to record the temperature dependence of the position of the absorption bands of  $\text{CH}_{2\text{as}}$  and  $\text{CH}_{2\text{s}}$ . For example, the effect of vitamin  $\text{D}_2$  in the presence of  $\text{Mg}^{2+}$  ions was studied in [33]: it was found that the phase transition is significantly slowed down, however, the shape of the curves remains uniform, which indicates the ordering effect of the molecule on the bilayer, accompanied by a decrease in the fraction of *trans* conformers (Fig. 6). As an auxiliary source of

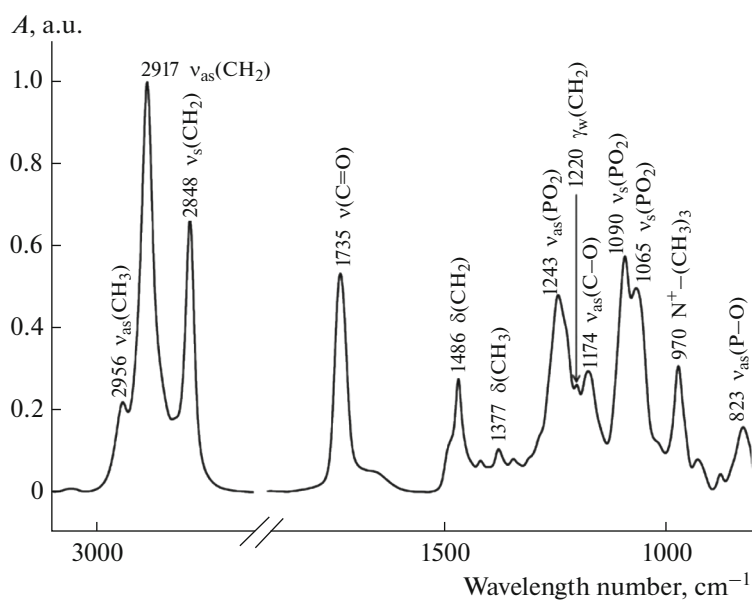


Fig. 5. Normalized IR spectrum of attenuated total internal reflection of dipalmitoylphosphatidylcholine.

information, the authors used the width of this absorption band (at the level of 0.75 peak height), which decreased with the introduction of vitamin D<sub>2</sub> into liposomes, which confirms the data of the thermogram.

However, for multicomponent liposomes prone to microphase formation, for example, containing 80% DPPC and 20% CL, the shape of thermograms can significantly change in the presence of drug molecules. For control unloaded vesicles, the curve is smooth, S-shaped (Fig. 7), individual microphases do not differ. In [18], the effect of independent interaction of moxifloxacin with microphases of different CL contents was detected, which is reflected by a funda-

mental change in the shape of the curve position of CH<sub>2as</sub> vs. temperature, namely, the minima in the temperature range of 28–35°C, indicating local ordering of the bilayer (Fig. 7).

A widespread approach is the mathematical processing of spectra by the principal component method, which can also provide additional information on the phase transition of liposomal formulations of drug molecules, especially in the case of accumulation of a large amount of data. In [38], interaction of fluphenazine with egg sphingomyelin liposomes was considered. A fine analysis of the spectral changes allowed the authors to conclude that the inclusion of the drug in the bilayer leads to a decrease in the phase

**Table 2.** Characteristic bands in the IR spectrum of lipids; vibration types are abbreviated as val., valent; def., deformation; sc., scissor-like; pend., pendular; as., asymmetrical; s., symmetrical; wag., wagging

Wavelength, cm <sup>-1</sup>	Vibration	Wavelength, cm <sup>-1</sup>	Vibration
3010	=C–H (val.)	1378	CH <sub>3</sub> (s. def.)
2956	CH <sub>3</sub> (as. val.)	1400–1200	CH <sub>2</sub> (wag.)
2920	CH <sub>2</sub> (as. val.)	1228	PO <sub>2</sub> <sup>-</sup> (as. val.)
2870	CH <sub>3</sub> (s. val.)	1170	CO–O–C (as. val.)
2850	CH <sub>2</sub> (s. val.)	1085	PO <sub>2</sub> <sup>-</sup> (s. val.)
1730	C=O (val.)	1070	CO–O–C (sym. val.)
1485	(CH <sub>3</sub> ) <sub>3</sub> N <sup>+</sup> (as. def.)	1047	C–O–P (val.)
1473, 1472, 1468, 1463	CH <sub>2</sub> (sc.)	972	(CH <sub>3</sub> ) <sub>3</sub> N <sup>+</sup> (as. val.)
1460	CH <sub>3</sub> (as. def.)	820	P–O (as. val.)
1405	(CH <sub>3</sub> ) <sub>3</sub> N <sup>+</sup> (s. def.)	730, 720, 718	CH <sub>2</sub> (pend.)



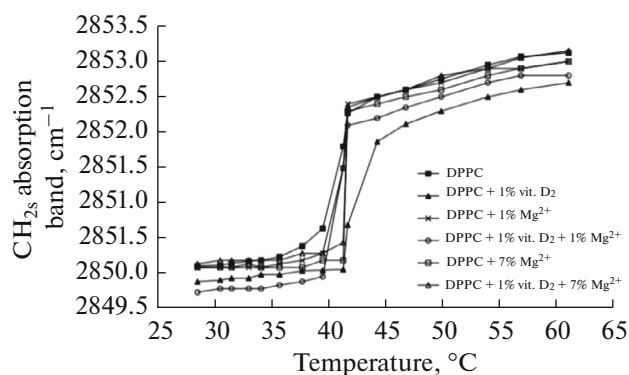


**Fig. 6.** Position of the absorption band of  $\text{CH}_2$  stretching vibrations in DPPC liposomes in the presence of vitamin  $\text{D}_2$  and  $\text{Mg}^{2+}$  ions.

transition temperature in proportion to the content of the drug molecule, which in turn leads to rapid release of fluphenazine into the aqueous phase.

The IR spectroscopy method is sensitive to changes in the packing density of acyl chains in the case of external action on the membrane, for example, under the vibrational–rotational motion of magnetite nanorods in a low-frequency nonheating alternating magnetic field [11]. Deconvolution of the observed absorption band, that is, decomposition into several components, made it possible to quantify the effect of loosening the bilayer.

The absorption bands of the carbonyl and phosphate groups are primarily sensitive to changes in the degree of hydration of these functional groups, spe-

cifically due to the formation of ionic bonds and aggregation.

Hydrated carbonyl  $\text{C}=\text{O}$  group in lipids and liposomes absorbs at  $1730\text{ cm}^{-1}$ . A partially negative charge is present on oxygen, which in free liposomes is compensated by the formation of hydrogen bonds with water molecules. With a decrease in the degree of hydration, that is, breaking of part of the hydrogen bonds, the characteristic wave number increases. This happens, for example, in the interaction of liposomes with polycations or a number of biologically active polar substances [7, 34]. Changes in the absorption region of the carbonyl group are extremely informative when analyzing changes at the lipid–water interface, including for monitoring liposome preservation during storage [7].

For the phosphate group, two main absorption bands were determined, corresponding to symmetric ( $1088\text{ cm}^{-1}$ ) and asymmetric ( $1250\text{--}1230\text{ cm}^{-1}$ ) stretching vibrations. Of greatest interest is the band of asymmetric vibrations, as more sensitive to the degree of hydration. The low-frequency shift of the position of this absorption band is associated with an increase in the degree of hydration [34], and vice versa. The appearance and shape of this band can significantly change with the addition of a drug molecule, as shown in [35] using liposomes with nonsteroidal anti-inflammatory drugs included in them.

In addition to analyzing the shift of the absorption bands of the carbonyl and phosphate groups, the deconvolution procedure can be extremely useful, since it becomes possible to identify the components corresponding to the functional groups associated with the drug molecule. For example, when doxorubi-

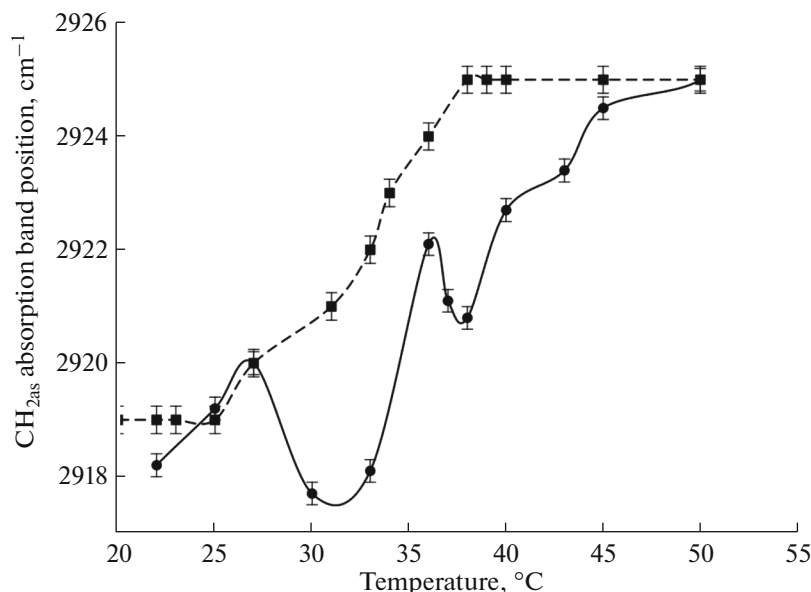


**Fig. 7.** Position of the absorption band of the stretching vibrations of  $\text{CH}_2$  in the DPPC–cardiolipin, 8 : 2, liposomes (dashed line) and liposomes of the same composition loaded with moxifloxacin.

**Table 3.** Information derived from main absorption bands in the IR spectrum of liposomes

Absorption band	Information derived	Possible methods to analyze the spectra	Refs.
CH <sub>2as</sub> , CH <sub>2s</sub>	Effect of the drug molecule on lipid packing density	Analysis of the position of absorption bands (shift to higher wavelength numbers indicates loosening, and lower numbers, ordering of the bilayer)	[11, 33]
	Effect of the drug on phase transition	Analysis of the CH <sub>2as</sub> (T) and CH <sub>2s</sub> (T) thermograms; principal component analysis	[11, 18, 33]
CO	Effect of the drug on the interface; formation of H bonds with cationic ligands	Analysis of the position of absorption bands (shift to higher wavelength numbers indicates higher hydration and to lower numbers, formation of electrostatic bonds)	[7]
		Deconvolution of the absorption bands for quantitative assessment of changes in the hydration rate of the carbonyl group	[7, 34, 36, 37]
PO <sub>2as</sub>	Effect of the drug on the hydrophilic surface of liposomes	Analysis of the position of absorption bands (shift to higher wavelength numbers indicates formation of electrostatic bonds)	[26, 35]
		Deconvolution of the absorption bands for quantitative assessment of changes in the hydration rate of the phosphate group	[34]

cin modified with a spermine and stearic acid fragment is inserted into anionic liposomes, there is a two-fold decrease in the proportion of highly hydrated phosphate groups corresponding to the component at 1219 cm<sup>-1</sup> and a twofold increase in the proportion of low hydrated carbonyl groups (1745 cm<sup>-1</sup> component) [34].

Thus, the IR spectroscopy method is informative in the study of many parameters of liposomal systems: the phase transition process, electrostatic interaction with drugs, and changes in the microenvironment at the lipid–water interface due to binding to ligands or during aggregation. Table 3 shows the main methods for processing liposome absorption bands and information that can be obtained.

**Methods on a chip** [39] are only gaining popularity for studying the interaction of the surface of liposomes with a drug. The giant plasmon resonance method is well suited for this. The authors first proposed to adsorb liposomes with different cholesterol content onto an alkane-modified dextran matrix on a chip, and then inject the drug into an external solution. The method involves utilization of the response of the system to the binding of a drug to a liposome membrane on a chip. An important role is played by the kinetics of sorption, through which conclusions can be drawn about the strength of the interaction of the drug with the membrane. Thus, it was found that anionic drugs quickly dissociate from the surface of liposomes, while cationic drugs, depending on their nature, are more strongly bound to the bilayer.

**Microscopy methods.** The size of monolamellar liposomes (30–150 nm) is much smaller than the dif-

fraction limit; therefore, electron microscopy and atomic force microscopy methods can be used to study the interaction of vesicles with drug molecules [40]. The specificity of these methods allows one to study the topology of the surface of the vesicles. An extensive review of liposome imaging methods is presented in [41]. Here, we would like to highlight the features of the microscopy methods applied to studies of the effect of drug loading on liposome morphology.

The advantages of AFM include the ability to work in both contact and noncontact mode and obtain information about the morphology of liposomes without additional sample preparation (staining, fixing, or labeling). However, cantilever movements can cause bilayer deformation [42], and the vesicles themselves must be deposited on a substrate, which may affect their morphology [41].

The applicability of the AFM method for 3D analysis of a population of liposomes loaded with doxorubicin was shown in [43]: vesicles with the largest crystals of doxorubicin took an elongated shape; data were confirmed by cryoelectron microscopy.

The applicability of scanning electron microscopy for liposomal systems is limited due to structural changes under high vacuum. However, it is the electron microscopy methods that make it possible to determine not only the size of the vesicles, but also to evaluate their lamellarity. Negative contrasting, for example with UO<sub>2</sub>(CH<sub>3</sub>COO)<sub>2</sub>, may be useful for evaluation. Moreover, the need for drying, fixing, and staining the sample also makes it difficult to obtain reliable results. The solution to this problem was pro-

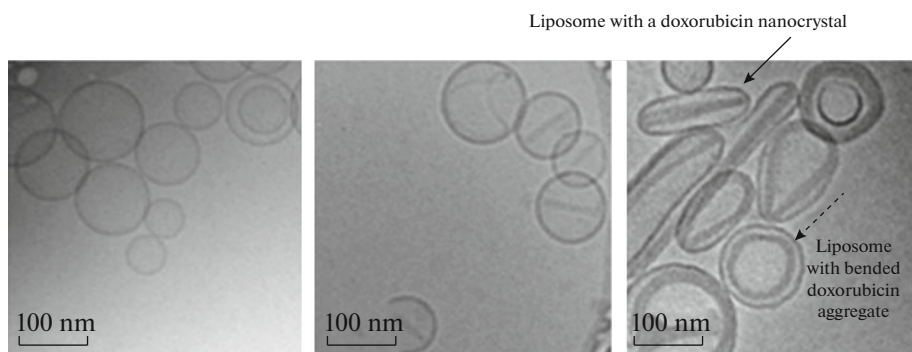


**Fig. 8.** Cryoelectron microscopy of (left to right) control unloaded liposomes, liposomes containing 20 mol. % doxorubicin, and liposomes containing 40 mol % doxorubicin.

posed by Danilatos, the author of the method of ESEM (environmental scanning electron microscopy), which allows working with samples in a gaseous environment, including air.

Cryoelectron microscopy plays a deservedly significant role in visualization and characterization of liposomal forms of drugs (Fig. 8). The method allows one to study liposomes in their native state, without the use of additional fixation or staining procedures. Depending on the thickness of the sample, a resolution of up to 5 nm can be achieved [41]. This method allows tracking the effect of the molar ratio of the drug molecule and lipids on the morphology of vesicles, as in [44]: at a molar ratio of 0.05, liposomes are expected to resemble coffee beans with a doxorubicin nanocrystal inside, but high molar ratios (0.37), even triangular structures were unexpectedly found in which three nanocrystals of doxorubicin formed a regular triangle within one liposome.

In case the loaded drug does not form a crystalline form in the liposome, cryoelectron microscopy can also be useful. Thus, in [45], the increased electron density of the inner cavity of liposomes compared to images of control unloaded vesicles allowed to evaluate the incorporation of vincristine, vinblastine, and vinorelbine into the inner cavity of liposomes.

Recently, in the laboratory of Prof. Barenholz, an approach to reconstruct the 3D structure of liposomes from 2D cryoelectronic micrographs was proposed [46]; it allows obtaining additional information on the distribution of the drug in the vesicles. This approach can be extremely useful in studying the interaction of liposomes with, for example, lipophilic-modified drugs, which can distort the structure of the membrane.

**Free electron laser diffraction method.** Exceptional results were achieved upon imaging of liposomes loaded with doxorubicin in solution by the method of free electron laser diffraction (coherent diffraction imaging using free electron laser diffraction) [47]. According to the diffraction pattern from single loaded liposome, the authors were able to reconstruct the real

shape of the doxorubicin crystal in the aqueous cavity of liposomes. This method is so far limited in use, since not all drugs form crystals in liposomes, but can be extremely useful in studying the incorporation of nanocrystals into vesicles.

#### *Methods to Study Lipid Systems Requiring the Introduction of Additional Labels*

**Fluorescence labeling methods.** An important role in the study of the structure of liposomes and their complexes is played by fluorescence spectroscopy. Since natural lipids do not have intrinsic fluorophores in the structure, it is necessary to introduce reporter tags into vesicles, depending on the properties of which it is possible to obtain information on the state of the hydrophobic or hydrophilic part of liposomes [48]. A number of key properties of fluorescent labels can be formulated, which should be considered when choosing:

(1) The main characteristics of fluorophores, namely the wavelengths of excitation and emission, quantum yield and fluorescence lifetime;

(2) Often, for the study of lipid systems, preference is given to labels whose fluorescence properties change dramatically with a change in the polarity of the medium;

(3) The simplicity of the technique for incorporating a fluorescent label into liposomes is desirable, and localization of the label in the vesicle should be verified.

A reliable and convenient label for liposomes is pyrene, by changing the fluorescence spectrum of which one can judge the change in the mobility of the hydrophobic chains of lipids (Fig. 9).

One of the first works in which it was proposed to use pyrene to study the state of the hydrophobic part of the bilayer is [49]. The authors compared a number of organic molecules—pyrene, naphthalene, and 1,12-benzperylene—from the point of view of their behavior in the bilayer, including during the phase transition. Completion of the phase transition has been found to

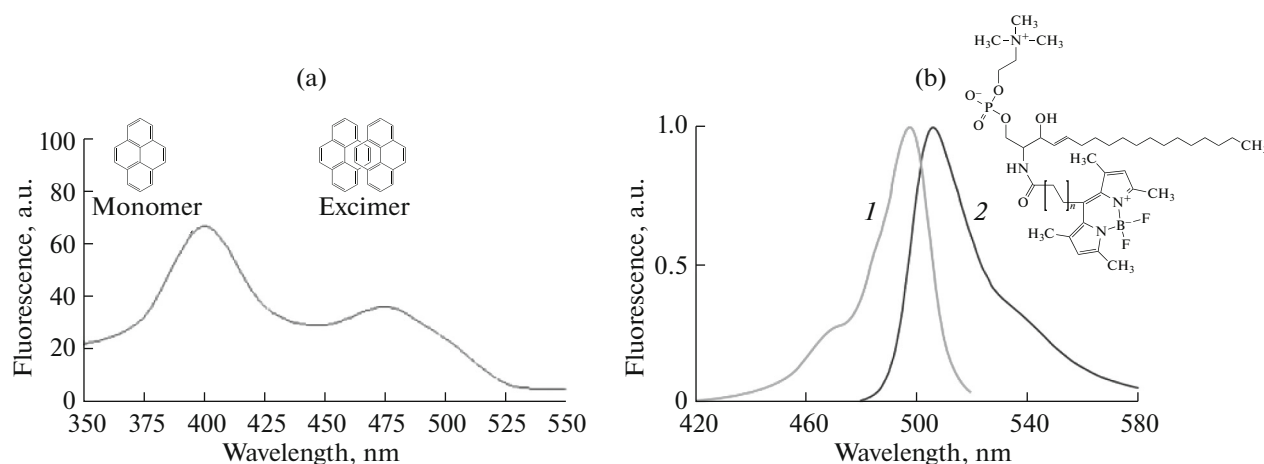


**Fig. 9.** Fluorescent reporter labels to study the state of the hydrophobic part of the bilayer. (a) Fluorescence spectrum of pyrene; monomer and excimer formulas are given. (b) Structure and absorption spectra (1) and fluorescence (2) of *N*-[7-(4,4-difluoro-1,3,5,7-tetramethyl-4-boron-3 $\alpha$ ,4 $\alpha$ -diazos-indexan-8)heptyl]sphingosine-1-phosphatidylcholine.

lead to a deepening of the pyrene in the bilayer. A similar effect was found for 1,12-benzperylene, while naphthalene remained unchanged.

In the fluorescence spectrum of pyrene there are two maxima: 394 (monomer) and 475 nm (excimer dimer consisting of an excited and unexcited pyrene molecule). Further studies [50] showed that the ratio of the intensities of these maxima is an analytically significant value. When the membrane is loosened, the probability of excimer formation increases, which leads to a proportional increase in the intensity of the corresponding maximum. In [51], it was shown, for example, that binding of some antiarrhythmic agents (ethmosin, xantiverin) to liposomal membranes is accompanied by a decrease in the microviscosity of the bilayer. However, the same work also noted the weakness of pyrene as labels: the signals from monomer or excimer often overlap with the signals from the drugs themselves, which makes the calculation of the relationship unreliable.

Promising is the use of intensely fluorescent labels based on borofluoride dipyrrolylmethylene (BODIPY) complexes (Fig. 9). For more efficient incorporation of such labels into liposomes, lipid-like molecules carrying the BODIPY fragment are often synthesized. Significant progress in the synthesis of such molecules was achieved by the laboratory of Prof. Vodovozova E.L. Thus, a lipid-like label was obtained [52], which has a high extinction coefficient  $\epsilon = 90000$  and is embedded in the hydrophobic part of the bilayer. The use of such labels greatly simplifies the analysis, for example, in the study of protein–membrane interactions [52], but a number of features of this approach should be taken into account. The label provides information about its closest microenvironment, while microphase separation is often observed for liposome complexes with polyelectrolytes; the data in this case may be difficult to analyze. Moreover, for reliable integration of the

label into the bilayer, its lipophilic modification is required; without this, it is possible to move the label along the bilayer in the process of, for example, a phase transition.

**Fluorescence correlation spectroscopy.** The FCS method is based on the fact that the diffusion of fluorescent molecules causes fluctuations in the fluorescence intensity in a small unit volume (0.1–0.5 fL), which is created in a confocal microscope (Fig. 10). This method allows one to obtain information on the local concentration of biomolecules, as well as to monitor aggregation, interaction with ligands, translational diffusion, and internal mobility of fluorescently labeled biopolymers. The measured quantity is the radiation intensity  $F(t)$  from several fluorescent objects in the laser illuminated volume. The intensity fluctuation is due to the Brownian motion of fluorescent objects in the laser illuminated volume. The time during which a given object crosses the illuminated volume is related to the diffusion coefficient  $D$  [53]. To calculate  $D$ , and later on the hydrodynamic radius, the autocorrelation function  $G(t)$  is analyzed (5):

$$G(t) = \frac{\langle I \rangle^2 + \langle \delta I(t) \delta I(t + \tau) \rangle}{\langle I \rangle^2}, \quad (5)$$

where  $I(t)$  is the fluorescence intensity at time  $t$ ;  $I(t + \tau)$ , fluorescence intensity after a period of time  $\tau$ .

An analysis of the autocorrelation function  $G(t)$  determines the translational diffusion time,  $\tau_d$ , which characterizes the residence time of a molecule in the unit volume considered (6):

$$G(\tau) = \frac{1}{N(1 + \tau/\tau_d)(1 + (\tau/a^2\tau_d))^{1/2}}. \quad (6)$$

The method is referred to single molecule detection methods, since it allows working with minimal

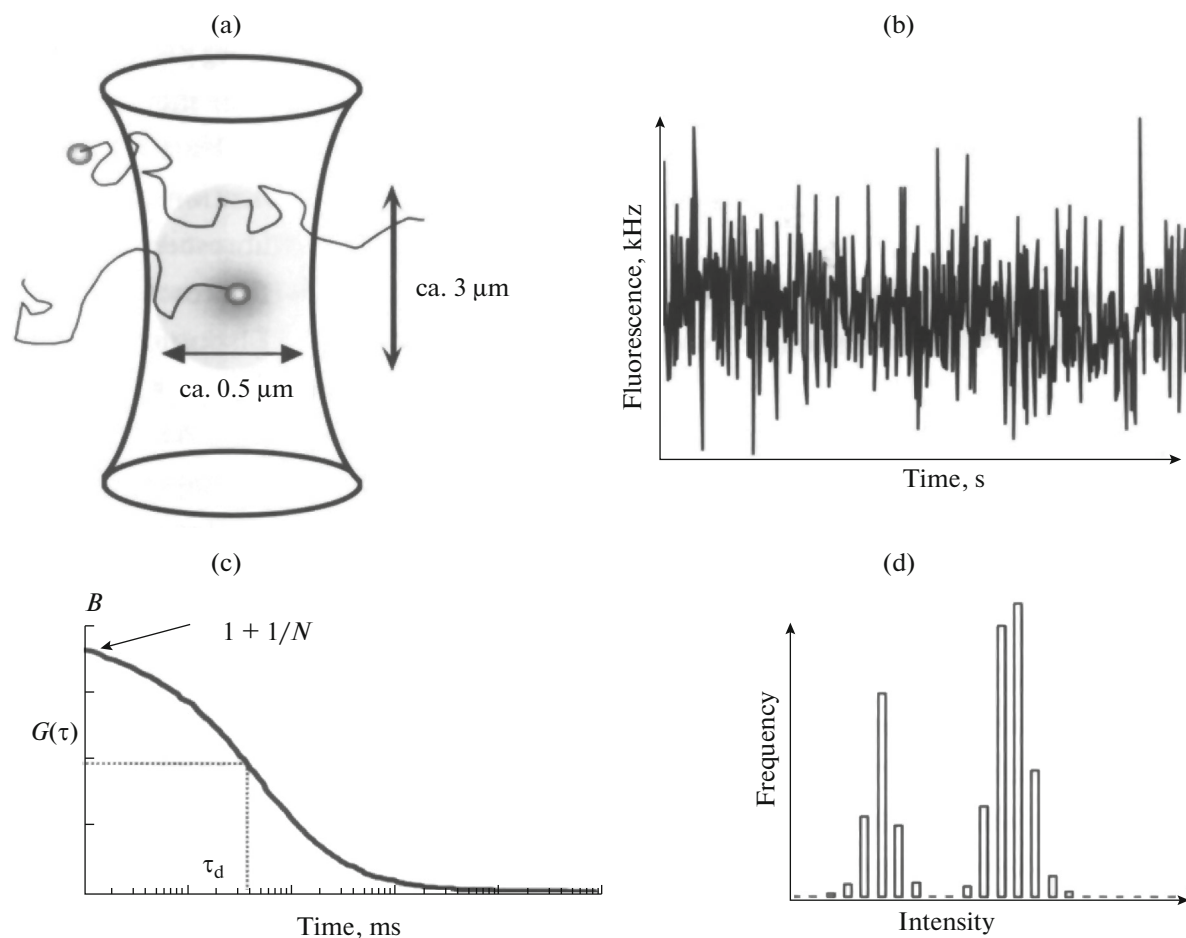


**Fig. 10.** The principle of fluorescence correlation spectroscopy. (a) Focused laser beam illuminates a fixed small volume of the measured system (1 fL). (b) Measurement of fluctuation of the fluorescence intensity in the detection volume (0.1–0.5 fL) as a function of time. (c) Analysis of the intensity autocorrelation allows to determine the average number of particles in the detection volume and translational diffusion time of the studied fluorescent molecules. (d) Statistical analysis of the distribution of particle molecular brightness (the number of detected fluorescence photons per molecule per second).

fluorophore concentrations (single molecules in the illuminated volume).

FCS is especially informative if the drug itself is a fluorophore. For example, the work [54] examined the interaction of the well-studied antifungal drug sanguinarine, for which antitumor activity was recently discovered, with a lipid bilayer. The diffusion coefficient of sanguinarine incorporated into liposomes ( $63.8 \pm 3 \mu\text{m}^2 \text{s}^{-1}$ ) is seven times lower than that for a drug in a buffer solution ( $9.07 \pm 0.42 \mu\text{m}^2 \text{s}^{-1}$ ). In contrast, the introduction of beta-cyclodextrin, an oligosaccharide capable of interacting with the bilayer, led to an increase in  $D$  by almost a factor of five ( $25.76 \pm 1.21 \mu\text{m}^2 \text{s}^{-1}$ ). Damage to the liposomal membrane under the influence of beta-cyclodextrin leads to significantly greater mobility of the drug molecule, which is reflected in the FCS signal.

If the drug is not a fluorophore, an appropriate label can be introduced, and its concentration may be minimal in view of the fact that FCS can be referred to

single-molecule detection methods. The change in  $D$  is judged by the viscosity of the liposomes; a significant change indicates softening or, conversely, hardening of the bilayer.

A large number of works in recent years have been devoted to the FCS method for analyzing the interaction of liposomal dosage forms with blood plasma proteins. For example, the behavior of a liposomal form of fluorescently labeled di- $\beta$ -D-galactopyranoside in the presence of serum albumin, transferrin, apolipoprotein A1, and fibrinogen was considered in [55]. The authors used FCS to track the release of liposomal content (for this, galactosidase was introduced into the external solution during the release experiments, which cleaved the bond between fluorescein and galactopyranoside, after which free fluorescein was determined by FCS) and to calculate the dissociation constants of the complex with proteins. For this, it was necessary to use proteins labeled with the Alex 488 dye, which are titrated with a liposomal suspension.



Protein binding leads to a change in the FCS signal; mathematical data processing can even allow calculating the dissociation constants of the complexes.

**Time-resolved anisotropy (TRA).** Time-resolved anisotropy is a relatively new microspectroscopic method widely used to study the structure of biomolecules and their complexes in solutions. It allows one to monitor the rotational dynamics of both a complex of biomolecules and each of the fragments with independent rotation, and as a result, obtain detailed information on the spatial structure of liposomal systems [53, 56, 58].

In a TRA experiment, the value of fluorescence anisotropy is determined as a function of time [57]. The anisotropy of spherical molecules whose rotation is symmetric (isotropic) decays according to the monoexponential law; in the general case, the “decay” of anisotropy is described by the multiexponential dependence (7):

$$r(t) = \sum \beta_j \exp(-t/\varphi_j), \quad (7)$$

where  $\varphi_j$  are the individual rotation correlation times, reflecting the rotational speed of the fluorophore, and  $\beta_j$  are the contributions of the corresponding components to the anisotropy decay.

Since the anisotropy  $r(t)$  is calculated from the difference between the observed components of the fluorescence emission  $I_{\parallel}(t)$  and  $I_{\perp}(t)$ , reliable values of the anisotropy  $r(t)$  can be calculated only for the cases when significant fluorescence emission is observed. For this reason, fluorophores with a decay time comparable to the estimated correlation rotation time are usually chosen as labels. If the fluorescence lifetime  $\tau$  is much shorter than  $\varphi$ , then the fluorescence intensity decays before a noticeable loss of anisotropy occurs.

In biosystems, there are several reasons for the loss of anisotropy (or depolarization): the rapid movement of the fluorescent label relative to its attachment site, the slower internal movement of the biopolymer segments, the slow rotation of the entire biopolymer molecule, the very slow rotation of the supramolecular complex, as well as the energy transfer between chromophores. In the interaction of liposomal forms of drugs with proteins, for example, blood proteins, the decline in anisotropy takes on a complex form: additional sources of depolarization appear, associated with the rotation of the entire complex and/or its individual segments, which is reflected in the appearance of corresponding correlation rotation times.

TRA is applicable for studying both homogeneous and microheterogeneous and heterogeneous systems [53, 58]. Consider several examples of the study of supramolecular structures based on liposomes by TRA.

In [59], the behavior of the antifungal drug itraconazole was studied using liposomes labeled with 1,6-diphenyl-1,3,5-hexatriene. Using a combination of fluorescence and molecular dynamics methods, the authors showed that a drug molecule can cause bilayer

ordering, reducing the mobility of hydrophobic chains.

The interaction of the surface protein of bacteriophage M13 with small monolamellar vesicles of dimyristoylphosphatidylcholine–dimyristoylphosphatidic acid (80 : 20 by weight) was studied by the TRA. Fluorescence was monitored by tryptophan residue of the protein [60]. The decrease in anisotropy is characterized by two correlation rotation times. The short correlation time  $\varphi_1$  (0.5 ns) reflects the rapid depolarization process inside the protein fragment, and the long,  $\varphi_2$  (more than 20 ns), corresponds to the rotation of the entire liposome system containing the protein ( $\varphi_{\text{protein} + \text{liposome}}$ ). There is no correlation rotation time corresponding to rotation of free protein, which indicates complete binding of the protein to the liposome.

In [61], using the methods of TRA and FCS, the change in the state of the lipid bilayer during the oxidation of fatty acids was studied. Using a fluorescent analog of a phospholipid BP-C11, which is able to be incorporated into the lipid bilayer, the change in lipid packing density (by the molecular mobility of the label in the bilayer through the correlation rotational times) was determined during the oxidation of unsaturated fatty acids (arachidonic acid) in the model phospholipid. During the oxidation of arachidonic acid, the lipid bilayer became significantly less mobile. A similar conclusion was obtained from the analysis of FCS data using a fluorescent label monopirenylphosphatidylcholine, where there was a slowdown in lateral diffusion during lipid oxidation in the same liposome system. As a result, the molecular action for changing the structure of the bilayer during lipid peroxidation of biomembranes was determined.

**EPR spectroscopy** provides valuable information about the nature, ground state of paramagnetic centers, and their immediate surroundings. Paramagnetic centers include atoms and molecules with an odd number of electrons, ions having partially filled internal electron shells, free radicals, and point defects in solids.

The use of EPR spectroscopy for studying biosystems is limited, since there are few natural paramagnetic centers in such objects. Speaking about the investigation of the interaction of liposome membranes with drugs, it is advisable to consider the types of spin labels intended for introduction into the bilayer. Then the information obtained from the EPR spectrum of the label can be used to analyze the fluidity of the membrane and detection of defects in it.

The structure of the EPR spectrum is complex, but modern methods of mathematical modeling make it possible to calculate the expected spectra. The interaction of an electron only with an external magnetic field leads to a single line in the EPR spectrum, one should take into account the interaction of the electron's magnetic moment with the magnetic moment of nearby nuclei, the so-called hyperfine interaction

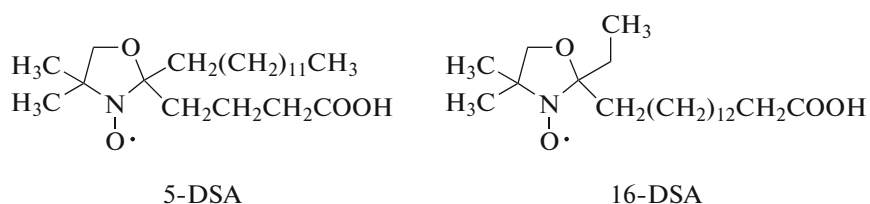


Fig. 11. The structure of 5-DOXYL-stearic acid (5-DSA) and 16-DOXYL-stearic acid (16-DSA).

(HFI), which leads to additional splitting of the spectral lines of paramagnetic systems in a magnetic field (the so-called hyperfine splitting, HFS).

The correlation time of rotational diffusion and the HFI constant are the main quantitative parameters in the spectra of reporter labels for liposomes.

An obvious limitation of the applicability of the EPR spectroscopy method for the analysis of liposome systems is the following technical fact. EPR spectrometers that record the signal from powder samples are most common, however, the correct interpretation of such results for liposome systems is difficult; it is necessary to search for methods for recording spectra from liquid samples. There are special cells based on capillaries, for example, the Bruker AquaX system, which requires a small sample volume (18–30  $\mu\text{L}$  per cm of the capillary system), however, such installations are extremely rare. This fact probably explains the relatively rare use of such a valuable method as EPR spectroscopy for the analysis of liposome systems.

Labels most often contain a nitroxyl radical (Fig. 11). The behavior of iminonitroxyl radicals in a lipid bilayer is well studied: it is believed that they rotate like spinners with axial symmetry [62].

5-DOXYL-stearic acid (5-DSA) and 16-DOXYL-stearic acid (16-DSA) became the “favorite” spin labels in the study of liposomal systems, since in aggregate the information from these two labels describes well the subpolar (5-DSA) and hydrophobic sections (16-DSA) of the bilayer. The change in the viscosity of the membrane can be estimated from the change in the HFS  $2A_{\text{max}}$  value (Fig. 12) in the spectra of liposomes labeled with 5-DSA, since it reflects the rotational mobility of lipid molecules. It is known that  $2A_{\text{max}}$  increases with decreasing membrane viscosity [63]. From the spectra of 16-DSA labeled liposomes, the rotational correlation time  $\tau$  was calculated from the spectrum parameters  $W_0$ ,  $h_0$ , and  $h_1$  (Fig. 12) according to Eq. (8):

$$\tau = (6.5 \times 10^{-10}) W_0 \left[ \left( \frac{h_0}{h_1} \right)^{0.5} - 1 \right]. \quad (8)$$

An increase in rotational correlation time also indicates a decrease in the viscosity of the bilayer.

Analysis of both of these parameters showed that the incorporation of paclitaxel into the DPPC liposomes causes an increase in the viscosity of the bilayer [63], which can be used not only to create new dosage forms, but also to better understand how active molecules interact with the membrane.

The label can be metal ions, for example, copper [64], and metal ions are introduced at the stage of dispersion of the thin lipid film. The change in the intensity of the EPR spectrum signal and the calculated values of the spin Hamiltonian made it possible to more accurately establish the structure of a liposome preparation CPX-351 containing cytarabine and daunorubicin: copper ions in the parallel plane bind to the former molecule, and in the perpendicular, to the latter one. It was found that daunorubicin forms complexes with copper in stoichiometry 1 : 1 or 2 : 1.

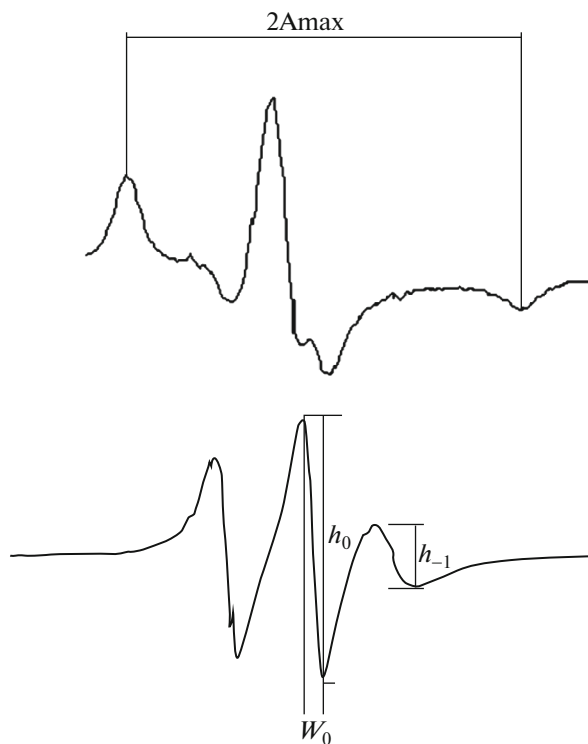


Fig. 12. Typical EPR spectrum of 5-DSA- and 16-DSA-labeled liposomes of dipalmitoylphosphatidylcholine.

**Table 4.** Comparison of the methods to study the mechanisms of interaction between liposomes and drugs

Methods	Chain mobility	Phase transition temperature	Morphology	Electrostatic interaction	Interactions with plasma proteins	Morphology of crystals inside liposomes
IR spectroscopy	+	+		+	+	
Fluorescence methods	+			+	+	
EPR spectroscopy	+					
DSC		+		+		
SAXS						+
Free electron diffraction						+
Methods on chip				+	+	
Microscopy methods			+			+

## CONCLUSIONS

How drugs interact with the biomembrane is the most important issue that faces the development of new biocompatible forms of drugs with improved biopharmaceutical characteristics. This is primarily due to the fact that a significant proportion of active molecules, in particular anti-inflammatory nonsteroid drugs and most antibiotics, have considerable side effects, including phototoxicity, hemodynamic disturbances, thrombosis, hepatotoxicity, and neurotoxicity. In some cases, the development of side effects is due to the nature of the drug itself, which, in addition to affecting the target in the body, causes nonspecific changes in the cell membrane. Such an effect was found, for example, for nonsteroidal anti-inflammatory drugs [35]: the interaction of active molecules with acyl chains causes the membrane to loosen and form defects in it. For antibacterial drugs of the fluoroquinolone class, using mixed anionic liposomes as an example, it was shown that moxifloxacin causes a redistribution of lipids in the bilayer and the formation of hexagonal mesophases. Such changes can lead to a violation of the integrity of the cell membrane, an increase in thrombogenicity, and other side effects.

The methods described in this review allow us to deeply study the mechanisms of interaction of drugs with a lipid bilayer and to reveal the fine structure of liposomal formulations of drug molecules depending on their chemical nature and composition of the lipid matrix. However, each method when used alone does not provide a complete picture of the ongoing process. Therefore, the issue of a combination of methods is relevant. Table 4 provides a brief summary of the

information that can be obtained from a particular method. The most informative methods stand out: IR spectroscopy and a group of fluorescence methods. These methods provide a wide range of possibilities when studying the state of a biomembrane during phase transitions and in the interaction of a lipid bilayer with drug substances. When studying supramolecular ensembles based on liposomes, the methods of FCS and TRA are extremely informative, allowing us to obtain detailed information on the spatial structure and molecular mobility of both the entire complex based on liposomes and its individual components. Combining them with methods that provide information on the morphology of vesicles allows researchers to get a complete picture of the interaction of a drug molecule with a bilayer. It can be expected that in the near future the scope of the methods considered in the review, primarily IR spectroscopy and fluorescence methods for studying biological objects, will expand, since with the improvement of technical equipment, fundamentally new applications of these methods will become available, for example, the ability to track the dynamics of individual vesicles in solution.

## FUNDING

The work was supported by the Russian Foundation for Basic Research (project no. 18-33-00134).

## COMPLIANCE WITH ETHICAL STANDARDS

The work has no studies involving humans or animals as subjects of the study.

## Conflict of Interests

Authors declare they have no conflicts of interests.

## REFERENCES

1. Manaia, E.B., et al., *Int. J. Nanomed.*, 2017, vol. 12, pp. 4991–5011.
2. Kinuta, M. and Takei, K., *Cell Struct. Funct.*, 2002, vol. 27, no. 2, pp. 63–69.
3. Kulikov, K.G. and Koshlan, T.V., *Zh. Tekh. Fiz.*, 2015, vol. 85, no. 12, pp. 26–32.
4. Yaroslavov, A.A., et al., *Colloid J.*, 2011, vol. 73, no. 3, pp. 430–435.
5. Sanchez-Purra, M., et al., *Int. J. Pharm.*, 2016, vol. 511, no. 2, pp. 946–956.
6. Kinuta, M., et al., *Proc. Natl. Acad. Sci. U. S. A.*, 2002, vol. 99, no. 5, pp. 2842–2847.
7. Deygen, I.M. and Kudryashova, E.V., *Russ. J. Bioorg. Chem.*, 2014, vol. 40, no. 5, pp. 547–557.
8. Eremenko, A.V., et al., *Electroanalysis*, 2012, vol. 24, no. 3, pp. 573–580.
9. Deygen, I.M. and Kudryashova, E.V., *Colloids Surf.*, 2016, vol. 141, pp. 36–43.
10. Filipe, V., Hawe, A., and Jiskoot, W., *Pharm. Res.*, 2010, vol. 27, no. 5, pp. 796–810.
11. Le-Deygen, I.M., et al., *Nanomed. Nanotechnol.*, Biol. Med. Elsevier Inc., 2019, vol. 21, p. 102065.
12. Shin, M., et al., *Mol. Pharm.*, 2018, vol. 15, no. 3, pp. 721–728.
13. González-Rodríguez, M.L. and Rabasco, A.M., *Expert Opin. Drug Deliv.*, 2011, vol. 8, no. 7, pp. 857–871.
14. Yaroslavov, A.A., et al., *Adv. Colloid Interface Sci.*, 2008, vol. 142, nos. 1–2, pp. 43–52.
15. Smith, M.C., et al., *Anal. Bioanal. Chem.*, 2017, vol. 409, no. 24, pp. 5779–5787.
16. Kim, M.W., Niidome, T., and Lee, R., *Mar. Drugs*, 2019, vol. 17, no. 10, pp. 581–593.
17. Singh, S., *Int. J. Nanomed.*, 2018, vol. 13, pp. 11–13.
18. Le-Deygen, I.M., et al., *Chem. Phys. Lipids*, 2020, vol. 228, p. 104891.
19. Rouf, M.A., et al., *J. Liposome Res.*, 2009, vol. 19, no. 4, pp. 322–331.
20. Robson, R.J. and Dennis, E.A., *J. Phys. Chem.*, 1977, vol. 81, no. 11, pp. 1075–1078.
21. Biltonen, R.L. and Lichtenberg, D., *Chem. Phys. Lipids*, 1993, vol. 64, pp. 129–142.
22. Bilge, D., et al., *Spectrochim. Acta, A. Mol. Biomol. Spectrosc.*, Elsevier B.V., 2014, vol. 130, pp. 250–256.
23. Di Foggia, M., et al., *J. Therm. Anal. Calorim.*, 2017, vol. 127, no. 2, pp. 1407–1417.
24. Wei, X., et al., *Mol. Pharm.*, 2017, vol. 14, no. 12, pp. 4339–4345.
25. Li, T., et al., *J. Control. Release*, 2018, vol. 288, pp. 96–110.
26. Mady, M.M., et al., *Cell Biochem. Biophys.*, 2012, vol. 62, no. 3, pp. 481–486.
27. Perinelli, D.R., et al., *Int. J. Pharm. Elsevier*, 2017, vol. 534, nos. 1–2, pp. 81–88.
28. Pereira-Leite, C., et al., *J. Phys. Chem. B*, 2012, vol. 116, no. 46, pp. 13608–13617.
29. Cipolla, D., et al., *Pharm. Res.*, 2016, vol. 33, no. 11, pp. 2748–2762.
30. Cipolla, D., et al., *RSC Adv.*, 2016, vol. 6, no. 8, pp. 6223–6233.
31. Feng, L., et al., *Biomaterials*, 2018, vol. 181, pp. 81–91.
32. Kleinschmidt, J.H., *Lipid-Protein Interactions: Methods and Protocols*, New York: Humana Press, 2013.
33. Toyran, N. and Severcan, F., *J. Mol. Struct.*, 2007, vol. 839, nos. 1–3, pp. 19–27.
34. Deygen, I.M., et al., *Langmuir*, 2016, vol. 32, no. 42, pp. 10861–10869.
35. Manrique-Moreno, M., et al., *Biochim. Biophys. Acta*, 2009, vol. 1788, no. 6, pp. 1296–1303.
36. Lewis, R.N., et al., *Biophys. J.*, 1994, vol. 67, no. 6, pp. 2367–2375.
37. Manrique-Moreno, M., et al., *Lett. Drug Des. Discov.*, 2009, vol. 7, no. 1, pp. 50–56.
38. Kuć, M., et al., *Chem. Phys.*, 2015, vol. 458, pp. 9–17.
39. Baird, C.L., Courtenay, E.S., and Myszkowski, D.G., *Anal. Biochem.*, 2002, vol. 310, no. 1, pp. 93–99.
40. Ruozi, B., et al., *Int. J. Nanomed.*, 2011, vol. 6, pp. 557–563.
41. Robson, A.L., et al., *Front. Pharmacol.*, 2018, vol. 9, pp. 1–8.
42. Ruozi, B., et al., *Eur. J. Pharm. Sci.*, 2005, vol. 25, no. 1, pp. 81–89.
43. Takahashi, N., et al., *J. Pharm. Sci. Am. Pharm. Assoc.*, 2018, vol. 107, no. 2, pp. 717–726.
44. Johnston, M.J.W., et al., *J. Liposome Res.*, 2008, vol. 18, no. 2, pp. 145–157.
45. Zhigaltsev, I.V., et al., *J. Control. Release*, 2005, vol. 104, no. 1, pp. 103–111.
46. Shamrakov, D., et al., *Int. J. Pharm.*, 2018, vol. 547, nos. 1–2, pp. 648–655.
47. Chang, W.-H., et al., *Nanoscale*, 2018, vol. 10, no. 6, pp. 2820–2824.
48. Alves, A.C., et al., *Sci. Rep.*, 2017, vol. 7, no. 1, pp. 1–11.
49. Lianos, P., Mukhopadhyay, A.K., and Georghiou, S., *Photochem. Photobiol.*, 1980, vol. 32, no. 3, pp. 415–419.
50. Macdonald, A.G., et al., *Biochim. Biophys. Acta*, 1988, vol. 938, pp. 231–242.
51. Beregovaya, E.G., et al., *Biopolimery Kletka*, 1993, vol. 9, no. 5, pp. 19–26.
52. Boldyrev, I., et al., New BODIPY lipid probes for fluorescence studies of membranes, *J. Lipid Res.*, 2007, vol. 48, no. 7, pp. 1518–1532.
53. Kudryashova, E.V., *Funktsionirovanie i struktura belkov na poverkhnostyakh razdela faz. Novye metody issledo-*

- vaniya* (The Functioning and Structure of Proteins on Phase Interfaces: New Research Methods), Palmarium Academic Publishing AV Akademikerverlag GmbH and Co., 2013.
54. Paul, B.K., Ghosh, N., and Mukherjee, S., *Colloids Surf.*, 2018, vol. 170, pp. 36–44.
55. Mittag, J.J., et al., *Eur. J. Pharm. Biopharm.*, 2017, vol. 119, pp. 215–223.
56. Cundall, R.B. and Dale, R.E., *Time-Resolved Fluorescence Spectroscopy in Biochemistry and Biology*, Cundall, R.B. and Dale, R.E., Eds., New York: Plenum Press, 1983, pp. 555–605.
57. Krishnamoorthy, G., *J. Biosci.*, Springer India, 2018, vol. 43, no. 3, pp. 555–567.
58. Kudryashova, E.V., Gladilin, A.K., and Levashov, A.V., *Usp. Biol. Khim.*, 2002, vol. 42, pp. 257–294.
59. Poojari, C., et al., *Chem. Phys. Lipids*, 2019, vol. 223, p. 104784.
60. Van Slooten, M.L., et al., *J. Pharm. Sci.*, 2000, vol. 89, no. 12, pp. 1605–1619.
61. Borst, J.W., et al., *Biochim. Biophys. Acta—Mol. Cell Biol. Lipids*, 2000, vol. 1487, no. 1, pp. 61–73.
62. Ivanov, L.V. and Kartel', N.T., *Rep. Natl. Acad. Sci. Ukr.*, 2012, vol. 5, pp. 139–145.
63. Zhao, L., et al., *Int. J. Pharm.*, 2007, vol. 338, nos. 1–2, pp. 258–266.
64. Dicko, A., et al., *Int. J. Pharm.*, 2010, vol. 391, nos. 1–2, pp. 248–259.

*Translated by N. Onishchenko*